Biophysical Journal Volume 70 February 1996 868–877

The Interfacial Elastic Packing Interactions of Galactosylceramides, Sphingomyelins, and Phosphatidylcholines

Janice M. Smaby, Vitthal S. Kulkarni, Maureen Momsen, and Rhoderick E. Brown
The Hormel Institute, University of Minnesota, Austin, Minnesota 55912-3698 USA

ABSTRACT The interfacial elastic packing interactions of different galactosylceramides (GalCers), sphingomyelins (SMs), and phosphatidylcholines (PC) were compared by determining their elastic area compressibility moduli (C_s^{-1}) as a function of lateral packing pressure (π) in a Langmuir-type film balance. To assess the relative contributions of the lipid headgroups as well as those of the ceramide and diacylglycerol hydrocarbon regions, we synthesized various GalCer and SM species with identical, homogeneous acyl residues and compared their behavior to that of PCs possessing similar hydrocarbon structures. For PCs, this meant that the *sn*-1 acyl chain was long and saturated (e.g., palmitate) and the *sn*-2 chain composition was varied to match that of GalCer or SM. When at equivalent π and in either the chain-disordered (liquid-expanded) or chain-ordered (liquid-condensed) state, GalCer films were less elastic than either SM or PC films. When lipid headgroups were identical (SM and PC), C_s^{-1} values (at equivalent π) for chain-disordered SMs, but not chain-ordered SMs, were 25–30% higher than those of PCs. Typical values for fluid phase (liquid-expanded) GalCer at 30 mN/m and 24°C were 158 (±7) mN/m, whereas those of SM were 135 (±7) mN/m and those of PC were 123 (±2) mN/m. Pressure-induced transitions to chain-ordered states (liquid-condensed) resulted in significant increases (two- to fourfold) in the "in-plane" compressibility for all three lipid types. Typical C_s^{-1} values for chain-ordered GalCers at 30 mN/m and 24°C were between 610 and 650 mN/m, whereas those of SM and of PC were very similar and were between 265 and 300 mN/m. Under fluid phase conditions, the π-C_s^{-1} behavior for each lipid type was insensitive to whether the acyl chain was saturated or monounsaturated. Measurement of the C_s^{-1} values also provided an effective way to evaluate the two-dimensional phase transition region of SMs, GalCers, and PCs. Modest heterogeneity in the acyl composition led to transitional broadening. Our findings provide useful information regarding the in-plane elasticity of lipids that are difficult to investigate by alternative methods, i.e., micropipette aspiration technique. The results also provide insight into the stability of sphingolipid-enriched, membrane microdomains that are thought to play a role in the sorting and trafficking of proteins containing glycosylphosphatidylinositol anchors with cells.

INTRODUCTION

Interest in sphingolipids continues to grow because of newly discovered roles in important cell biological processes. Such roles include a requirement for sphingolipids in target membranes for fusion to occur with envelope viruses (Nieva et al., 1994), a major regulatory role in lipid signal transduction events pertaining to cell apoptosis (Hannun, 1994), as well as proposed roles in the sorting and trafficking of proteins bearing glycosylphosphatidylinositol (GPI) anchors via the formation of sphingolipid-enriched, membrane microdomains (Brown and Rose, 1992; Fiedler et al., 1993). Hence, determining the physicochemical parameters responsible for sphingolipids behaving differently from other membrane lipids is likely to be valuable for understanding these processes at the molecular level.

A particularly effective way to gain insight into the elasticity of lipids in bilayer model membranes is by the micropipette aspiration technique. This approach has provided information regarding various mechanical-elastic parameters of bilayers, including curvature or bending moduli as well as lateral area dilation moduli, which often are referred to as elastic moduli of area compressibility (e.g., Kwok and Evans, 1981; Evans and Needham, 1987, and references therein). The micropipette aspiration technique has provided valuable insights into the changes in the elastic packing interactions that occur in phosphatidylcholine bilayers as acyl chain composition is varied or as cholesterol is added (Needham et al., 1988; Needham and Nunn, 1990). However, because this approach requires that the lipids being studied form large, stable bilayer vesicles, its utility is restricted with respect to lipid type and mixing compositions. For these reasons, application to pure sphingolipids has not been possible, although equimolar mixtures of sphingomyelin and cholesterol have been investigated (Needham and Nunn, 1990; McIntosh et al., 1992).

An alternative means of investigating the in-plane elastic packing interactions of simple sphingolipids is by Langmuir film balance techniques. An important advantage of studying lipid-lipid interactions using the monolayer approach is that the range of molecular areas known to occur in membrane systems can be investigated systematically. In doing so, subtle alterations in intermolecular behavior can be

---

Received for publication 15 August 1995 and in final form 10 November 1995.

Address reprint requests to Dr. Rhoderick E. Brown, Hormel Institute, 801 16th Ave. NE, Austin, MN 55912-3698 USA. Tel.: 507-433-8804; Fax: 507-437-9606; E-mail: reb@maroon.tc.umn; Internet: rebrown@wolf.co.net.

The phase state denoted by L is liquid expanded (chain disordered); C is condensed (chain ordered); M is mixed phase state consisting of both liquid and condensed phases. All measurements were carried out at 24°C.

Portions of this investigation were presented at the 39th Annual Meeting of the Biophysical Society held in San Francisco, CA (Smaby et al., 1995).

0006-3495/96/02/868/10 $2.00

detected, while avoiding mesophasic structural changes that often occur in bilayer model membrane systems as the lipid phase state is changed. To date, investigators studying lipids usually have focused on lipid force-area behavior but have neglected to analyze the film balance data in terms of interfacial compressibility. In cases where sphingolipid interfacial compressibility values have been reported, they have been limited to only a few discrete surface pressures (Ali et al., 1991, 1993; Grönberg et al., 1991; Slotte et al., 1993; Smaby et al., 1994; Bittman et al., 1994).

Here, we compare the in-plane elastic packing interactions of different galactosylceramides (GalCers), sphingomyelins (SMs; ceramide-1-phosphocholine), and phosphatidylcholines (PCs) by determining their interfacial elastic moduli of area compressibility as a function of lateral packing pressure. Our results provide insight into the influence of the ceramide region of sphingolipids, the diacylglycerol region of glycerol-based phospholipids, and the polar headgroup of these lipids on their interfacial elasticity. We also use the interfacial elastic area compressibility moduli measurements to monitor the two-dimensional phase transition region of SMs, GalCers, and PCs. Assessment of the two-dimensional phase transition behavior of these lipids is important for quantitatively comparing their in-plane mixing interactions with other lipids such as cholesterol (e.g., Ali et al., 1994a; Smaby et al., 1994). For certain SMs (e.g., bovine and egg SM), this is not trivial, because of their subtle and broad phase transition behavior. Finally, this study provides a foundation for future investigations using interfacial elastic moduli of area compressibility measurements to evaluate the elastic packing interactions within various lipid mixtures (e.g., sterol-sphingolipid).

MATERIALS AND METHODS

With the exception of 1-palmitoyl-2-nervonoyl PC (PNPC), all phospholipids including egg and bovine SM were purchased from Avanti Polar Lipids (Alabaster, Al). Stock solutions were prepared by dissolving lipids in either petroleum ether/ethanol (95:5), hexane/ethanol (95:5), or hexane/isopropanol/water (70:30:2.5). The petroleum ether was purified as described earlier (Ali et al., 1991), the ethanol was distilled from zinc and KOH, and the hexane and isopropanol were purchased from Burdick Jackson Laboratories (Muskegon, MI).

Synthesis of 1-palmitoyl-2-nervonoyl-PC

The anhydride derivative of nervonic acid ($24{:}1^{\Delta 15(c)}$), prepared by the method of Selinger and Lapidot (1966), was reacted with 1-palmitoyl-2-hydroxy-phosphatidylcholine (lyso-PC) (Avanti Polar Lipids) in the presence of the catalyst 4-pyrrolidino pyridine (molar ratio of lyso-PC:fatty acid anhydride:catalyst, 1:5:1) in chloroform under nitrogen at 30°C for 18 h to yield 1-palmitoyl-2-nervonoyl-sn-glycero-3-phosphocholine (PNPC) (Mason et al., 1981). After removing the catalyst by acid extraction using $CHCl_3/CH_3OH$/0.1 N HCl (6:3:2.2), the lower phase was collected and dried. The crude PC product was then purified by flash column chromatography (230–400 mesh silica gel) using a step-gradient consisting of $CHCl_3/CH_3OH$ (85:15) and $CHCl_3/CH_3OH/H_2O$ (65:35:8). The pure product, PNPC, was recrystallized and freed of silica gel as described below for SM. The final stock concentration of PNPC, determined by dry weight on a Cahn microbalance (model 4700) and by phosphate analysis (Bartlett, 1959), matched to within 4%.

Synthesis of homogeneously acylated SMs

Egg sphingomyelin (Avanti Polar Lipids) was deacylated by hydrolyzing in methanolic HCl at 65–75°C for about 36 h (Cohen et al., 1984). The reaction product, sphingosylphosphocholine (SPC, lyso-sphingomyelin), was purified by flash column chromatography and recrystallized. Reacylation of the lyso SM was achieved by reacting with the *N*-hydroxy succinimide esters of desired fatty acids (Lapidot et al., 1967) in the presence of the catalyst *N*-ethyl di-isopropylamine at 60°C under nitrogen for 4 h (Schwarzmann and Sandhoff, 1987). After lyophilization, the reaction mixture was subjected to a Folch partition. The crude SM (Folch lower phase) was purified by flash column chromatography on 230–400-mesh silica gel using a step-gradient solvent system consisting of $CHCl_3/CH_3OH$ (85:15) and $CHCl_3/CH_3OH/H_2O$ (55:45:10). After pooling and drying the fractions containing pure SM by rotary evaporation, silica gel, which co-eluted with the lipid, was removed by Folch partitioning. Recrystallization of the lipid was achieved by dissolving in a minimum amount of hot $CHCl_3/CH_3OH$ (4:1), precipitating with cold acetone (−20°C), and collecting the precipitated lipid by low-speed centrifugation at 4°C. By following this procedure, we prepared *N*-oleoyl sphingosylphosphocholine (*N*-$18{:}1^{\Delta 9(c)}$) SPC or 18:1 SM), *N*-stearoyl sphingosylphosphocholine (*N*-18:0 SPC or 18:0 SM), *N*-palmitoyl sphingosylphosphocholine (*N*-16:0 SPC or 16:0 SM), and *N*-nervonoyl sphingosylphosphocholine (*N*-$24{:}1^{\Delta 15(c)}$) SPC or 24:1 SM). Final stock concentrations determined by dry weight on a Cahn microbalance (model 4700) and by phosphate analysis (Bartlett, 1959), matched to within 4%.

Synthesis of homogeneously acylated GalCers

Bovine brain GalCer (Avanti Polar Lipids) was deacylated by alkaline hydrolysis to obtain galactosylsphingoid (GalSpd or psychosine; deacylated GalCer with naturally occurring sphingoid base composition, usually sphingosine, 90%, and dihydrosphingosine, 10%) (Radin, 1974). Purification of the galactosylsphingosine (GalSph) fraction was achieved by medium pressure flash column chromatography on silica gel (230–400 mesh) using step gradients consisting of $CHCl_3/CH_3OH$ (85:15) and CH_3OH/iso-$CH_3CH_2CH_2OH$/2.5 M NH_4OH (10:65:25). The absence of the dihydro fraction of psychosine was confirmed by thin-layer chromatography using $CHCl_3/CH_3OH/H_2O/NH_4OH$ (70:30:4:1) as the solvent system (Radin, 1974). The *N*-hydroxy succinimide ester derivatives of desired fatty acids were prepared (Lapidot et al., 1967) and then reacted with GalSph in the presence of the catalyst *N*-ethyl di-isopropylamine at 60°C under nitrogen for 4 h (Schwarzmann and Sandhoff, 1987) to obtain homogeneously *N*-acylated GalSph. The reaction product (*N*-acylated GalSph) was purified by flash column chromatography on 230–400-mesh silica gel column using solvent system $CHCl_3{:}CH_3OH{:}H_2O$ (90:10:0.5). The final product was freed from traces of silica gel and recrystallized by the same procedure as described for SM derivatives. In this way, we prepared *N*-oleoyl galactosylsphingosine (*N*-$18{:}1^{\Delta 9(c)}$ GalSph or 18:1 GalCer), *N*-stearoyl galactosylsphingosine (*N*-18:0 GalSph or 18:0 GalCer), *N*-palmitoyl galactosylsphingosine (*N*-16:0 GalSph or 16:0 GalCer), and *N*-nervonoyl galactosylsphingosine (*N*-$24{:}1^{\Delta 15(c)}$ GalSph or 24:1 GalCer). Concentrations of stock solutions (dissolved in hexane:isopropanol:water, 70:30:2.5 v/v) were determined by dry weight using a Cahn microbalance (model 4700).

Analysis of lipid purity and fatty acyl composition

Lipid purity was analyzed by thin-layer chromatography and judged to be >99% using the solvent systems described by Ali et al. (1991) and Smaby et al. (1994). The acyl homogeneity of the synthesized lipids was determined by capillary gas-liquid chromatography after release and esterification of the fatty acyl moieties. Quantitative release of the amide-linked acyl chains was achieved by hydrolyzing 0.5 mg of each lipid in 1 ml of acetonitrile/0.5 M HCl (9:1; v/v) as described by Aveldaño and Horrocks (1983). The released free fatty acids were trans-esterified by reacting with methanolic-HCl reagent (Supelco, Bellefonte, PA) at 90°C for 1 h. After extracting the fatty acid methyl esters with hexane, analysis was achieved by gas-liquid chromatography (Hewlett-Packard 5840A) using a 0.25-μm capillary column (J and W Scientific, Folsom, CA) as described by Cleary et al. (1994). The analysis showed the acyl homogeneity of our synthetic GalCer, SM, and PC derivatives to be >99%. The acyl composition of egg SM consisted of 86% palmitate (16:0), 0.4% myristate (14:0), 4.8% stearate (18:0), 1.1% arachidate (20:0), 2.5% behenate (22:0), 1.0% lignocerate (24:0), and 4.2% nervonate ($24{:}1^{\Delta 15}$). The acyl composition of bovine brain SM consisted of 63% stearate (18:0), 2.4% palmitate (16:0), 6.6% arachidate (20:0), 9.2% behenate (22:0), 6.1% lignocerate (24:0), and 13% nervonate ($24{:}1^{\Delta 15}$). These acyl compositions varied somewhat from the values shown in Avanti's catalog.

Langmuir film balance conditions

Water for the subphase buffer was purified by reverse osmosis, mixed-bed deionization, adsorption on activated charcoal, and filtration through a 0.22-μm Durapore membrane (Millipore Corp., Bedford, MA). The subphase buffer consisted of 10 mM potassium phosphate, 100 mM NaCl, and 0.2% sodium azide at a pH of 6.6. The buffer was filtered through a Diaflo hollow-fiber filter with a 10 kDa cutoff (Amicon Corp., Danvers, MA) and stored under argon until use.

Surface pressure-molecular area-surface potential (π-A-ΔV) isotherms were measured using a computer-controlled Langmuir-type film balance as described previously (Ali et al., 1991, 1993). Data shown in the figures represent averages of three to six isotherms. The pure lipids and lipid mixtures were spread in 51.67-μl aliquots. Films were compressed at a rate of $\leq$4 Å^2/molecule/min after an initial delay period of 4 min. The subphase was maintained at 24 ± 1°C.

Monolayer isothermal compressibility at a given surface pressure (π) was calculated from π-A data using

$$k_\pi = (-1/A_\pi)(\mathrm{d}A/\mathrm{d}\pi)_\pi,$$

where A_π is the area per molecule at the indicated surface pressure and π is the corresponding surface pressure. For convenience, we analyzed our data in terms of the reciprocal of isothermal compressibility, i.e., elastic moduli of area compressibility (C_s^{-1}), because this facilitated comparisons with measurements made in bilayer systems (e.g., Evans and Needham, 1987; Needham and Nunn, 1990; McIntosh et al., 1992) and discussed later. We used a 100-point sliding window that utilized every fourth point to calculate a C_s^{-1} value before advancing the window one point. Each π-C_s^{-1} curve consisted of 200 C_s^{-1} values obtained at equally spaced molecular areas covering the surface pressure range of 1 to 40 mN/m. We plotted the $C_s{}^{-1}$ values on a log scale because two-dimensional lipid phase transitions could be viewed more clearly than when plotted on a linear scale.

RESULTS

The hydrocarbon structural motif in which sphingoid-based and glycerol-based lipids are most similar occurs when at least one acyl chain of the glycerol-based lipid is long and saturated (e.g., palmitate or myristate) (Smaby et al., 1994). This condition arises because the first three carbons in the 18-carbon sphingosine base of simple sphingolipids are configurationally equivalent to the glycerol backbone of glycerol-based phospholipids (for a review, see Hauser and Poupart, 1992). As a result, the entire sphingosine base chain in sphingolipids and the combined glycerol backbone and *sn*-1 chain of phospholipids are oriented similarly with respect to the lamellar interface and define the long axis of the respective molecules. Moreover, the sole acyl chain of a sphingolipid and the *sn*-2 chain of a phospholipid are configurationally similar and, for the most part, are oriented parallel to the molecular long axis because of a sharp bend that occurs at carbon 2 in these acyl chains (see Hamilton et al., 1993, and references therein). Accordingly, we compared the behavior of different *N-acyl* galactosyl sphingosines (GalCers), *N-acyl* sphingosylphosphocholines (SMs), and 1-palmitoyl-2-*acyl* phosphatidylcholines (PCs) in which the "*acyl*" groups were matched. By doing so, we were able to evaluate the degree to which headgroup effects (GalCer versus SM) and hydrocarbon effects (SM versus PC) modulate the in-plane, elastic packing interactions of these lipids.

To begin, we compared *N*-oleoyl galactosyl sphingosine ($18{:}1^{\Delta 9}$ GalCer), *N*-oleoyl sphingosylphosphocholine ($18{:}1^{\Delta 9}$ SM), and 1-palmitoyl-2-oleoyl phosphatidylcholine not only because of their hydrocarbon configurational similarities but also because of their known liquid-expanded (i.e., chain-disordered) behavior at all surface pressures below film collapse (Smaby et al., 1983, and references therein; Lund-Katz et al., 1988; Ali et al., 1991, 1994b; Smaby et al., 1994). This permitted evaluation of the elastic moduli of area compressibility (C_s^{-1}) as a function of surface pressure (π) at various liquid-expanded surface pressures, including those reported to approximate the pressures found in biological membranes (30–35 mN/m) (Demel et al., 1975; Evans and Waugh, 1977; Blume, 1979; Cevc and Marsh, 1987). Moreover, the C_s^{-1} values could be determined under conditions free of the influence of two-dimensional phase transitions to more ordered states.

Fig. 1 shows plots of π versus C_s^{-1} as well as traditional π-A isotherms. Because dioleoyl PC (di-$18{:}1^{\Delta 9}$ PC) had often been used in earlier film balance investigations as a representative liquid-expanded PC (Demel et al., 1967; Lund-Katz et al., 1988), we included this lipid as a control.

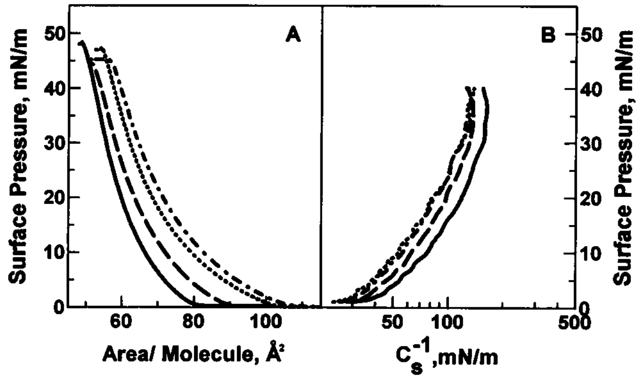

FIGURE 1 (*A*) Surface pressure versus molecular area isotherms and (*B*) surface pressure versus elastic moduli of area compressibility plots. Data were collected and calculated as described in Materials and Methods for $18{:}1^{\Delta 9}$ GalCer (——); $18{:}1^{\Delta 9}$ SM (– – –); 16:0, $18{:}1^{\Delta 9}$ PC (1-palmitoyl-2-oleoyl-*sn*-glycero-3-phosphocholine) (· · ·); and di-$18{:}1^{\Delta 9}$ PC (dioleoyl-*sn*-glycero-3-phosphocholine) (– · – · –).

As shown in Fig. 1 *A*, although all of the lipids did display liquid-expanded π-A isotherms, the observed molecular packing density at equivalent surface pressures was $18{:}1^{\Delta 9}$ GalCer > $18{:}1^{\Delta 9}$ SM > 16:0, $18{:}1^{\Delta 9}$ PC > di-$18{:}1^{\Delta 9}$ PC. Interestingly, the π-C_s^{-1} behavior (at equivalent surface pressures) showed just the opposite pattern in interfacial elasticity ($18{:}1^{\Delta 9}$ GalCer < $18{:}1^{\Delta 9}$ SM < 16:0, $18{:}1^{\Delta 9}$ PC = di-$18{:}1^{\Delta 9}$ PC), with the exception of the two PCs that displayed virtually superimposible behavior (Fig. 1 *B*). Hence, at 5 mN/m, C_s^{-1} values were 53 (±1), 46 (±1), and 40 (±1) mN/m for $18{:}1^{\Delta 9}$ GalCer, $18{:}1^{\Delta 9}$ SM, and 16:0, $18{:}1^{\Delta 9}$ PC (or di-$18{:}1^{\Delta 9}$ PC), respectively. However, upon reaching the physiologically relevant surface pressure of 30 mN/m, C_s^{-1} values roughly tripled to 158 (±9), 132 (±3), and 124 (±1) mN/m for $18{:}1^{\Delta 9}$ GalCer, $18{:}1^{\Delta 9}$ SM, and 16:0, $18{:}1^{\Delta 9}$ PC (or di-$18{:}1^{\Delta 9}$ PC), respectively.

To determine the extent to which the interfacial elasticity of GalCer, SM, and PC was affected by *cis* monounsaturation of the acyl chains, we synthesized GalCer and SM that had stearoyl instead of oleoyl acyl chains (see Materials and Methods). Fig. 2 shows both the π-A and π-C_s^{-1} behavior of these two sphingolipids as well as that of 1-palmitoyl-2-stearoyl PC (16:0, 18:0 PC) and distearoyl PC (di-18:0 PC). The π-A behavior of 18:0 GalCer was characteristic of a highly chain-ordered, condensed lipid film (Ali et al., 1993, 1994b). Indeed, the C_s^{-1} value at a surface pressure of 5 mN/m was 225 (±10) mN/m and was 648 (±8) mN/m at 30 mN/m (Fig. 2 B and Table 1). Replacing the galactose headgroup in 18:0 GalCer with phosphocholine to produce 18:0 SM had a "liquefying" effect on the interfacial behavior in that liquid-expanded behavior was evident at surface pressures below 7 mN/m (Fig. 2 *A*). Interestingly, the π-C_s^{-1} behavior in the liquid-expanded region ($1 < \pi < 7$ mN/m) ranged from 30 to 45 mN/m and was almost identical to values measured for $18{:}1^{\Delta 9}$ SM.

Above 7 mN/m, the π-A behavior showed a sharp inflection indicative of the onset of a two-dimensional phase transition to a more chain-ordered, condensed state. Not surprisingly, a sharp drop in C_s^{-1} values occurred at surface pressures between 7 and 10 mN/m before reversing sign and increasing to values more characteristic of a condensed phase at higher surface pressures. The dramatic drop in C_s^{-1} values reflects discontinuities in lateral packing at phase boundaries and accompanying lateral density fluctuations that are known to occur when liquid-expanded and liquid-condensed phases coexist (e.g., Phillips et al., 1975; Nagle and Scott, 1978; Mouritsen et al., 1989). For this reason, plots of π-C_s^{-1} proved to be an informative way to recognize the surface pressure range over which fluid (LE) and condensed (LC) phases coexist.

Interestingly, 18:0 SM achieved C_s^{-1} values in the range of 270 to 287 mN/m at surface pressures between 30 and 35 mN/m. These values were considerably lower than those observed at similar surface pressures with 18:0 GalCer, but were quite similar to those observed with 1-palmitoyl-2-stearoyl PC (16:0, 18:0 PC). The π-A and π-C_s^{-1} behavior of 16:0, 18:0 PC suggested that its LE-LC transition was just finishing between 1 and 6 mN/m before entering a condensed state, a phase quite similar to that of 18:0 SM in terms of in-plane elasticity (e.g., compare π-C_s^{-1} behavior above 20 mN/m in Fig. 2 *B*). We also determined the π-C_s^{-1} behavior of di-18:0 PC, which showed classic liquid-condensed π-A behavior (Fig. 2 *A*) and no evidence of a LE-LC phase transition between 1 and 40 mN/m (Phillips and Chapman, 1968; Demel et al., 1972). At $\pi > 25$ mN/m, the C_s^{-1} values were very similar to those observed for 16:0, 18:0 PC, or 18:0 SM.

To determine whether the behavior of the stearoyl derivatives of GalCer, SM, and PC was representative of how acyl chain saturation affects in-plane elasticity, we investigated the behavior of these same lipids after acylation with palmitate. Fig. 3 shows plots of the π-C_s^{-1} behavior as well as π-A isotherms. Like 18:0 GalCer, the π-A behavior of 16:0 GalCer showed no evidence of a two-dimensional phase transition and was characteristic of an ordered, con-

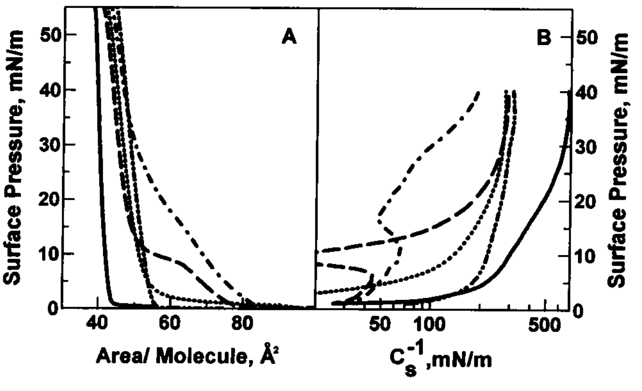

FIGURE 2 (*A*) Surface pressure versus molecular area isotherms and (*B*) surface pressure versus elastic moduli of area compressibility plots. Data were collected and calculated as described in Materials and Methods for 18:0 GalCer (——); 18:0 SM (– – –);16:0, 18:0 PC (1-palmitoyl-2-stearoyl-*sn*-glycero-3-phosphocholine) (· · ·); di-18:0 PC (distearoyl-*sn*-glycero-3-phosphocholine) (– · · · · · –); and bovine brain SM (– · – · –).

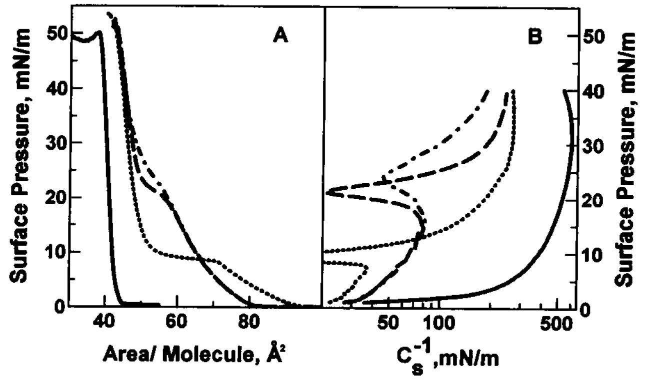

FIGURE 3 (*A*) Surface pressure versus molecular area isotherms and (*B*) surface pressure versus elastic moduli of area compressibility plots. Data were collected and calculated as described in Materials and Methods for 16:0 GalCer (——); 16:0 SM (– – –); di-16:0 PC (DPPC) (· · ·); and egg SM (– · – · –).

densed lipid film at high as well as low surface pressures (Ali et al., 1993, 1994b). Indeed, the C_s^{-1} value at a surface pressure of 5 mN/m was 279 (± 23) mN/m and exceeded 610 mN/m above surface pressures of 30 mN/m (Fig. 3 *B* and Table 1). Replacing the galactose headgroup in 16:0 GalCer with phosphocholine to produce 16:0 SM also had a "liquefying" effect on the interfacial behavior. This is clear from the LE-LC phase transition that occurred in 16:0 SM near 58 Å^2/molecule at 20 mN/m.

With respect to di-16:0 PC, our π-A isotherms were consistent with previous reports in that a distinct phase transition from a liquid-expanded to liquid-condensed (LE-LC) state was observed at 8.5 mN/m for dipalmitoyl-*sn*-glycero-3-phosphocholine (DPPC) (e.g., Phillips and Chapman, 1968; Müller-Landau and Cadenhead, 1979; Lund-Katz et al., 1988; Smaby et al., 1994). As is shown in Fig. 3 *B*, C_s^{-1} values for di-16:0 PC and 16:0 SM were low at liquid-expanded surface pressures and reflected the increased elasticity expected when the hydrocarbon chain packing is disordered, i.e., liquid expanded. Even so, sudden and dramatic decreases in C_s^{-1} values occurred in both di-16:0 PC and 16:0 SM films at the onset of the two-dimensional phase transition. With increasing π, C_s^{-1} values eventually reversed sign and increased to values more characteristic of the condensed phase. However, as with the stearoyl derivatives, the in-plane elasticity of condensed phase 16:0 SM or di-16:0 PC was greater than that of 16:0 GalCer.

Because palmitate accounts for 86% of the acyl residues in egg SM, its physicochemical properties have often been compared with those of di-16:0 PC (e.g., Lund-Katz et al., 1988; Smaby et al., 1994). In fact, the π-A isotherms of egg SM and *N*-palmitoyl SM reportedly are quite similar (Lund-Katz et al., 1988). Hence, we decided to determine whether π-C_s^{-1} plots would reveal differences between 16:0 SM and egg SM because 4% of egg SM's acyl chains are nervonoyl residues (see Materials and Methods). Fig. 3 shows both the π-A and π-C_s^{-1} behavior for 16:0 SM and egg SM. As reported previously (Smaby et al., 1994), egg SM displays a LE-LC transition with an onset pressure of 18 mN/m. However, in comparing the π-A behavior of egg SM and 16:0 SM (Fig. 3 *A*), we found that the two-dimensional phase transition of 16:0 SM was "sharper" than that of egg SM. Interestingly, plots of the π-C_s^{-1} behavior of these two lipids accentuated this somewhat subtle difference and provided insight into its occurrence. Fig. 3 *B* shows that the LE-LC phase transition region of egg SM is broader than that of 16:0 SM. Egg SM had a LE-LC transition that spanned about 17 mN/m, with onset occurring near 17 mN/m, attaining minimum C_s^{-1} near 24 mN/m, and ending near 34 mN/m. In contrast, 16:0 SM's LE-LC transition spanned about 11 mN/m, with onset occurring near 17 mN/m, attaining minimum C_s^{-1} near 22 mN/m, and ending near 28 mN/m (Fig. 3 B). To determine whether this was a general phenomenon that extended to other SMs as well, we compared the behavior of 18:0 SM and bovine brain SM, which contains 63% stearate and 13% nervonate residues (see Materials and Methods). Although significant differences in the π-A behavior of 18:0 SM and bovine brain SM had been reported by Yedgar et al. (1982), we found their bovine brain SM data to be unrealistic with respect to the known behavior of other SMs (Lund-Katz et al., 1988; Grönberg et al., 1991; Smaby et al., 1994). Our π-A data for bovine brain SM and 18:0 SM are shown in Fig. 2 *A*.

The π-C_s^{-1} behavior again proved useful for evaluating two-dimensional phase behavior of bovine brain SM and 18:0 SM (Fig. 2 *B*). The π-C_s^{-1} plot for bovine brain SM revealed its LE-LC transition to be quite broad, with onset occurring near 12 mN/m, attaining minimum C_s^{-1} near 16 mN/m, and ending near 34 mN/m. In contrast, 18:0 SM's LE-LC transition was "sharper" and much narrower (in a pressure sense) in that it spanned about 10.5 mN/m, with onset occurring near 6.5 mN/m, attaining minimum C_s^{-1} near 10 mN/m, and ending near 17 mN/m (Fig. 2 *B*). Hence, it was clear that acyl chain inhomogeneity in the SMs had dramatic effects on film elasticity (e.g., compare C_s^{-1} values at 30 mN/m in Table 1).

To gain further insight into the effect on nervonoyl acyl residues on interfacial hydrocarbon ordering and elasticity, we investigated the π-C_s^{-1} behavior of *N*-nervonoyl galactosylsphingosine (24:1$^{\Delta 15}$ GalCer), *N*-nervonoyl sphingosylphosphocholine (24:1$^{\Delta 15}$ SM), 1-palmitoyl-2-nervonoyl PC (16:0, 24:1$^{\Delta 15}$ PC), and dinervonoyl PC (di-24:1$^{\Delta 15}$ PC). The nervonoyl species of GalCer and SM were of particular interest because, as pointed out above, they are the predominant unsaturated species found in bovine brain GalCer as well as in bovine and egg SM. Furthermore, in certain mammalian cell membranes, the nervonoyl species can account for up to 55% of the total SM present (Barenholz and Thompson, 1980). Although this laboratory and another had previously reported the π-A behavior of 24:1$^{\Delta 15}$ GalCer (Ali et al., 1993, 1994b; Johnston and Chapman, 1988) and dinervonoyl-*sn*-glycero-3-phosphocholine (Smaby et al., 1994), no such data were available for either 24:1$^{\Delta 15}$ SM or 16:0, 24:1$^{\Delta 15}$ PC. Fig. 4 shows both the π-A as well as π-C_s^{-1} behavior for all four lipids. Unlike their "oleoyl" counterparts, the "nervonoyl" species all showed evidence of two-dimensional phase transitions. However, compared to 24:1$^{\Delta 15}$ GalCer's broad, metastable LE-LC transition that began near 65 Å^2/molecule at 10 mN/m, 24:1$^{\Delta 15}$ SM's transition was much less distinct, with onset occurring near 60 Å^2/molecule at 32 mN/m. Hence, changing the headgroup from galactose to phosphocholine "liquefied" sphingolipid behavior in an isothermal sense. In contrast, keeping the phosphocholine headgroup fixed while altering the hydrocarbon structure to 1-palmitoyl-2-nervonoyl glycerol resulted in distinct but relatively modest changes in two-dimensional behavior relative to 24:1$^{\Delta 15}$ SM's behavior. The LE-to-LC transition of 16:0, 24:1$^{\Delta 15}$ PC also began near 60 Å^2/molecule but at a slightly lower surface pressure (28 mN/m). For comparison, we also included the π-A isotherm of dinervonoyl PC (di-24:1$^{\Delta 15}$ PC), which we reported previously (Smaby et al., 1994).

TABLE 1 Lipid interfacial elastic moduli of area compressibility

	Π = 5 mN/m			Π = 30 mN/m		
Lipid	Phase state*	Molecular area (Å^2)	C_s^{-1} (mN/M)	Phase state*	Molecular area (Å^2)	C_s^{-1} (mN/m)
16:0 SM	L	71.0 ± 1.2	47.5 ± 0.5	M	47.2 ± 0.7	196.0 ± 6.1
18:0 SM	L	68.3 ± 0.4	43.3 ± 0.9	C	45.3 ± 0.3	268.9 ± 4.3
18:1 SM	L	79.0 ± 0.7	47.2 ± 2.0	L	58.7 ± 1.0	134.5 ± 7.3
24:1 SM	L	81.1 ± 0.7	50.5 ± 1.1	M	59.7 ± 0.9	104.9 ± 5.5
ESM	L	71.1 ± 0.4	47.8 ± 0.4	M	48.3 ± 0.1	98.3 ± 5.0
BSM	L	75.0 ± 0.5	48.8 ± 0.7	M	50.0 ± 0.4	100.1 ± 1.2
16:0 GalCer	C	42.5 ± 1.0	279.4 ± 23	C	40.3 ± 1.0	611.1 ± 17
18:0 GalCer	C	42.7 ± 0.4	225.1 ± 9.6	C	40.2 ± 0.3	647.7 ± 8.3
18:1 GalCer	L	71.9 ± 1.3	53.7 ± 1.1	L	55.8 ± 0.6	158.7 ± 6.6
24:1 GalCer	L	72.4 ± 1.4	47.7 ± 3.0	C	38.0 ± 0.7	341.7 ± 53
16:0, 16:0 PC	L	78.1 ± 1.2	32.3 ± 0.4	C	46.2 ± 0.7	264.5 ± 3.5
16:0, 18:0 PC	M	53.5 ± 1.1	59.7 ± 10	C	46.3 ± 0.9	278.8 ± 6.8
18:0, 18:0 PC	C	53.8 ± 0.4	184.8 ± 13	C	48.6 ± 0.3	299.3 ± 10
16:0, 18:1 PC	L	88.3 ± 0.6	39.6 ± 0.7	L	62.2 ± 0.8	122.9 ± 1.9
16:0, 24:1 PC	L	90.0 ± 0.5	39.2 ± 0.9	M	61.0 ± 0.3	48.7 ± 15
18:1, 18:1 PC	L	92.7 ± 1.1	40.5 ± 1.1	L	65.6 ± 1.1	116.6 ± 3.8
24:1, 24:1 PC	L	84.5 ± 0.6	33.4 ± 0.7	C	48.6 ± 0.4	231.0 ± 5.0

*Phase state denoted by L is liquid expanded (chain disordered); C is condensed (chain ordered); M is mixed phase state consisting of both liquid and condensed phases. All measurements were carried out at 24°C.

The π-C_s^{-1} behavior of 24:1$^{\Delta15}$ GalCer, 24:1$^{\Delta15}$ SM, 16:0, 24:1$^{\Delta15}$ PC, and di-24:1$^{\Delta15}$ PC showed behavior consistent with the occurrence of LE-LC phase transitions for each lipid. As can be seen in Fig. 4 *B*, sharp drops in C_s^{-1} values occurred at surface pressures and molecular areas where the π-A behavior showed inflections indicative of the onset of a two-dimensional phase transition. With increasing π (Fig. 4 *B*), C_s^{-1} values eventually reversed sign and increased to values more characteristic of the condensed phase. This can be seen clearly for 16:0, 24:1$^{\Delta15}$ PC. In the cases of 24:1$^{\Delta15}$ GalCer and di-24:1$^{\Delta15}$ PC (to a slight extent), the "surface pressure overshoot" observed in the LE-LC transition region (see π-A plots; Fig. 4 *A*) is clearly evident in the π-C_s^{-1} behavior (Fig. 4 *B*) and confirms the metastable behavior that we previously observed (Ali et al., 1993; Smaby et al., 1994). In the case of 24:1$^{\Delta15}$ SM (Fig. 4 B), there is evidence from the drop in C_s^{-1} values that the LE-LC transition begins near 30 mN/m but is not complete by 40 mN/m. Hence, the occurrence of a two-dimensional phase transition in the 24:1$^{\Delta15}$, but not the 18:1$^{\Delta9}$ derivatives, indicates that lengthening the monounsaturated acyl chain does have an ordering effect on all three lipid types, most likely because of increased van der Waals attractive forces.

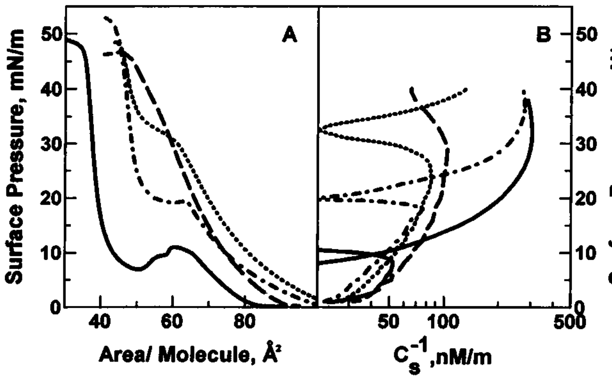

FIGURE 4 (*A*) Surface pressure versus molecular area isotherms and (*B*) surface pressure versus elastic moduli of area compressibility plots. Data were collected and calculated as described in Materials and Methods for 24:1$^{\Delta15}$ GalCer (——); 24:1$^{\Delta15}$ SM (– – –); 16:0, 24:1$^{\Delta15}$ PC (PNPC) (· · ·); and di-24:1$^{\Delta15}$ PC (dinervonoyl-*sn*-glycero-3-phosphocholine) (– · – · –).

DISCUSSION

It is clear that measurements of the interfacial elastic area compressibility moduli (C_s^{-1}) provide valuable insights into the in-plane elastic packing interactions of sphingolipids that are difficult, if not impossible, to obtain by alternative methods. In one such method, the micropipette aspiration technique (which was briefly described in the Introduction), measurements of the membrane area dilation in response to incremental changes in surface tension permit analysis of bulk compressibility moduli for lipid bilayers (e.g., Evans and Needham, 1987). However, because this approach is only amenable to lipids (or lipid mixtures) that form stable, single-walled, bilayer vesicles, it cannot be used to study many lipids, including certain sphingolipids. For instance, Needham and Nunn (1990) and McIntosh et al. (1992) were able to measure the bulk compressibility moduli of bovine brain SM and 24:0 SM only if these lipids were mixed with an optimal amount of cholesterol. Hence, to date, no comprehensive measurements of this type have been reported for pure SMs or GalCers.

An alternative method that provides limited insight into the elasticity of bilayers involves the reversible extraction of water from multilamellar lipid/water phases by osmotic stress (Parsegian et al., 1979). Although this method is well known for providing information about the hydration forces that occur at the bilayer surface, what is less appreciated is the fact that the same osmotic stress that pushes multilamellar bilayers together also acts to deform them laterally, resulting in a decrease in molecular cross-sectional area, which causes the bilayers to thicken. Although this method has been used in the past to evaluate the lateral compressibility of different lipids dispersed as multilamellar suspensions (Lis et al., 1982), it is now generally acknowledged to be fairly insensitive for the reasons detailed by Rand et al. (1988) and by Rand and Parsegian (1992).

This is not to imply that the monolayer approach is without limitations. For instance, we find that accurate experimental measurement of C_s^{-1} is possible up to surface pressures of approximately 35 mN/m, depending somewhat on the lipid under study. C_s^{-1} values at higher pressures cannot be obtained directly from the data and must be extrapolated by fitting the force-area isotherms to a monolayer equation of state (Smaby and Brockman, 1991; Feng et al., 1994). This inherent limitation appears to be related to intrinsic experimental factors such as trough composition and design.

Aside from these experimental limitations, another unresolved issue relates to the proper way to quantitatively compare monolayer and bilayer data. This issue has remained a subject of controversy for over 20 years. Many but not all investigators have concluded that monolayer surface pressures in the 30–35 mN/m range produce conditions similar to those found in each half of the bilayer (e.g., Demel et al., 1975; Evans and Waugh, 1977; Blume, 1979; Cevc and Marsh, 1987). Hence, we believe that the lipid C_s^{-1} values determined at 30 mN/m should provide a reasonable approximation of how lipid structural manipulations affects their elastic packing interactions in bilayers (Table 1). Unfortunately, none of the lipids investigated here have been studied by micropipette aspiration techniques. The only similar case for which we can compare monolayer data with micropipette aspiration bilayer data involves 16:0, $18{:}1^{\Delta 9}$ PC and 18:0, $18{:}1^{\Delta 9}$ PC data. Our monolayer C_s^{-1} value of 16:0, $18{:}1^{\Delta 9}$ PC at 30 mN/m (24°C) is 123 (±2) mN/m, whereas the unstressed bilayer value for 18:0, $18{:}1^{\Delta 9}$ PC at 15°C is 200 (±13) mN/m (Evans and Needham, 1987). However, it should be pointed out that the elastic moduli obtained for bilayers by micropipette aspiration actually include not only an area dilation parameter but also an elastic bending or curvature parameter. This latter parameter dominates when low tensions (2–3 $\times 10^{-3}$ mN/m) are applied, whereas the area dilation parameter dominates when applied tensions are increased by another 2 to 3 orders of magnitude. The net effect is that the "high tension" bilayer measurements contain not only the area dilation modulus but also a small contribution from the bending or curvature modulus (Evans and Rawicz, 1990). This latter contribution does not enter into the monolayer data. In any case, it is clear that more work will be needed to assess exactly how useful monolayer compressibility data will be for defining the equilibrium parameters that relate fluid monolayers and bilayers.

What the interfacial elastic moduli of area compressibility measurements reveal about the in-plane interactions of GalCers, SMs, and PCs

Based on our results, we can make the following generalizations about the relative behavior of GalCer, SM, and PC. When at equivalent π in either the chain-disordered (liquid-expanded) or chain-ordered (liquid-condensed) states, GalCer films are less elastic than either SM or PC films. This conclusion is based on the data presented here as well as previous data reported for GalCer derivatives (Ali et al., 1993). The higher packing density of GalCer compared to SM is especially interesting because the ceramide structures of the derivatives have been "matched" in the present study. Hence, it is clear that the galactose headgroup diminishes the elasticity among GalCer molecules more so than the phosphocholine headgroup does among SM molecules. Indeed, differing hydrated bulk volume and average orientation of these two headgroups are likely contributors to these differences in molecular packing elasticity (e.g., Ali et al., 1993, and Discussion therein). The smaller, less hydrated headgroup of GalCer would permit closer intermolecular approach than is possible with the larger, more hydrated phosphorylcholine headgroup and, in doing so, might enhance the potential for intermolecular hydrogen bonding, especially in the chain-ordered, condensed state (Bunow and Levin, 1980; Pink et al., 1988).

Interestingly, when the headgroups are identical (SM and PC), the C_s^{-1} values (at equivalent surface pressures) for chain-disordered SMs, but not chain-ordered SMs, are 25–30% higher than those for PCs. This generalization is based on comparison of SMs and PCs that were "matched" with respect to hydrocarbon structural configuration such as 16:0, $18{:}1^{\Delta 9}$ PC and $18{:}1^{\Delta 9}$ SM, 16:0, $24{:}1^{\Delta 15}$ PC and $24{:}1^{\Delta 15}$ SM, as well as di-16:0 PC and 16:0 SM (see Smaby et al., 1994; Hamilton et al., 1993, and references within). The higher C_s^{-1} values of the SMs compared to the PCs (at equivalent π in the liquid-expanded range) are likely to be a reflection of the specific chemical groups characteristic of the ceramide and diacylglycerol regions, respectively. In particular, the presence of amide linkages and hydroxyl groups in simple sphingolipids provides the capacity to be both hydrogen bond donors and acceptors, whereas the presence of ester linkages in glycerolipids provides only hydrogen bond accepting capability (for reviews, see Barenholz and Thompson, 1980; Thompson and Tillack, 1985). The structural ramifications for sphingomyelin may be restriction of the average orientation of the phosphorylcholine headgroup (and thereby affect the packing elasticity). Other investigators have noted SM's ability to form intramolecular hydrogen bonds (Barenholz and Thompson, 1980) and detected measurable effects on headgroup conformation by NMR (Bruzik, 1988).

Another intriguing aspect of liquid-expanded SMs is that their π-C_s^{-1} behavior is insensitive to whether the acyl chain is saturated or monounsaturated, as is indicated by their superimposible π-C_s^{-1} plots. This was also found to be the case for liquid-expanded GalCers when we compared the π-C_s^{-1} plots of 18:1$^{\Delta9}$ GalCer with data calculated for earlier 10:0 GalCer results (Ali et al., 1993). This feature was not limited to sphingolipids. The liquid-expanded portions of DPPC isotherms also displayed superimposible π-C_s^{-1} plots with 16:0, 18:1$^{\Delta9}$ PC. However, even more surprisingly, we found that the π-C_s^{-1} behavior of 16:0, 18:1$^{\Delta9}$ PC was very similar to that of di-18:1$^{\Delta9}$ PC. Hence, in terms of altering in-plane elastic packing interactions, introduction of a *cis* double bond into the middle of the *sn*-1 chain had no measurable effect on a PC that was already disordered (i.e., liquid-expanded) by virtue of *cis* unsaturation in the *sn*-2 chain (e.g. 16:0, 18:1$^{\Delta9}$ PC). The fact that di-18:1$^{\Delta9}$ PC and 16:0, 18:1$^{\Delta9}$ PC display very similar π-C_s^{-1} behavior is consistent with recent NMR results (Holte et al., 1995, and references therein). In these studies, Gawrisch and co-workers found that, at a given absolute temperature, the introduction of *cis* unsaturation into the *sn*-2 chains leads the adjacent *sn*-1 chains to become more disordered, despite the fact that highly unsaturated chains themselves are thought to be quite ordered structures (Applegate and Glomset, 1991). Hence, the gain in order brought about by increasing the *cis* double bond content of the *sn*-2 chain is somewhat but not entirely compensated by the decrease in order that occurs in the saturated *sn*-1 chain.

Interestingly, at equivalent surface pressures, chain-ordered SMs have C_s^{-1} values very similar to those of PCs if they are "matched" with respect to hydrocarbon structure (e.g., 16:0 SM and di-16:0 PC; 18:0 SM and 16:0, 18:0 PC). The absolute values of C_s^{-1} for chain-ordered lipids must be viewed with reservation because of the kinetic parameters associated with the formation of "true equilibrium" chain-ordered states (Phillips and Hauser, 1974). Nonetheless, because all of the lipids investigated in this study were treated in the same manner, it is reasonable to assume that the relative changes do provide useful insights.

The change in elasticity brought about by a two-dimensional phase transition produces C_s^{-1} values that are two- to fourfold higher in the chain-ordered (condensed) state than in the chain-disordered (liquid-expanded) state. Interestingly, a similar change in elastic compliance is predicted by certain statistical mechanical models based on mean-field, Ising-model, and Landau theory as the bilayer state goes from liquid to solid phase (Marcelja, 1974; Jähnig, 1981; also reviews by Caille et al., 1980; Nagle, 1980), as well as by Monte Carlo simulations involving the 10-state Pink model (Zuckermann et al., 1993) .

It is clear that even modest heterogeneity in the acyl composition leads to two-dimensional transitional broadening. Compared to bovine and egg SM, considerably higher C_s^{-1} values were observed at 30 mN/m for 18:0 SM and 16:0 SM, which are the major species of bovine brain and egg SM, respectively. We believe that 24:1 SM, which accounts for 13% of the bovine SM and for 4% of the egg SM, is the primary reason for the broader transitional behavior of bovine and egg SM. Aside from being a "contaminant," 24:1 SM shows a two-dimensional phase transition with an onset near 30 mN/m and 60 Å^2/molecule (Fig. 5 *B*). Hence, broadening of the transition regions of bovine and egg SM to higher surface pressures is not surprising. Indeed, our calorimetric scans of egg SM reveal its thermotropic melting behavior to be relatively broad, with onset and completion temperatures spanning over 15°C (unpublished observation). Other researchers also have noted broad thermotropic transitional behavior in bovine brain SM (e.g., Döbereiner et al., 1993).

Recognizing when fluid LE phase coexists with chain-ordered LC phase can be challenging because of the sometimes subtle and broad phase transition behavior of certain SMs. Whereas transition onset is generally (but not always) evident from π-A isotherms (see 24:1 SM), determining the transition completion pressure usually is more difficult. Examining the lipid π-C_s^{-1} behavior provides an effective way to approximate the transition onset and completion pressures. Knowing the transition behavior of SMs (and other lipids) is useful for accurately defining their mixing interactions with other lipids such as cholesterol (Ali et al., 1994a; Smaby et al., 1994). Failure to recognize these "transition effects" occasionally has led to misinterpretation of cholesterol's area condensation of SMs compared with PCs in earlier studies (see Smaby et al., 1994, Discussion).

Implications

The normal physiological mode by which mammalian cells adjust the physical properties of their membranes in response to external stimuli is by changing lipid composition. The two most common ways by which cells alter their lipid composition are by modifying lipid molecular structure or by adjusting cholesterol content. In this study, we have shown how structural modifications of sphingolipids affect their in-plane elastic packing interactions. It is interesting to note that the structural motifs typical for naturally occurring GalCers and SMs involve high levels of saturated acyl chains, whereas the typical structure for PC is one in which the sn-1 chain is saturated but the *sn*-2 chain is unsaturated. As a consequence, naturally occurring GalCers and SMs often are in more rigid, less elastic, chain-ordered states at physiological temperature compared to naturally occurring PCs, which generally are in less rigid, more elastic, chain-disordered states. These fundamental differences in hydrocarbon structure are likely to have important consequences with respect to the lateral organization of these lipids in biological membranes. Indeed, in recent cell biological studies, sphingolipid-enriched microdomains have been proposed to play roles in the concentrating and sorting of proteins bearing GPI anchors (Brown and Rose, 1992). These sphingolipid-enriched domains along with GPI-anchored proteins and certain kinases of the *Src* family colocalize in a low-density, insoluble fraction upon detergent treatment of cell membranes (e.g., Brown, 1993). The sphingolipid microdomains have been shown to be enriched in sphingomyelin, glycosylceramides, and cholesterol (Brown and Rose, 1992). Based on our results, it appears quite plausible that the resistance to detergent solubilization exhibited by sphingolipid-enriched microdomains is largely a reflection of their rigid, relatively inelastic packing state compared to "typical" PC species, i.e., *sn*-1 chain saturated and *sn*-2 chain unsaturated. In future reports, we will describe the effect of changing cholesterol content on the elastic properties of the sphingolipids studied here.

We thank Howard Brockman for the use of the Langmuir film balance and for helpful comments regarding this report, Evan Evans for pointing out references regarding measurements of elastic area compressibility moduli in lipid bilayers, Margot Cleary and Fred Phillips for assistance with the capillary GC analyses of lipid acyl composition, and Kristi Hyland for synthesizing and purifying several of the sphingolipids.

This investigation was supported by USPHS grant GM45928 and the Hormel Foundation.

REFERENCES

Ali, S., H. L. Brockman, and R. E. Brown. 1991. Structural determinants of miscibility in surface films of galactosylceramide and phosphatidylcholine: effect of unsaturation in the galactosylceramide acyl chain. *Biochemistry.* 30:11198–11205.

Ali, S., J. M. Smaby, H. L. Brockman, and R. E. Brown. 1994a. Cholesterol's interfacial interactions with galactosylceramides. *Biochemistry.* 33:2900–2906.

Ali, S., J. M. Smaby, and R. E. Brown. 1993. Acyl structure regulates galactosylceramide's interfacial interactions. *Biochemistry.* 32: 11696–11703.

Ali, S., J. M. Smaby, and R. E. Brown. 1994b. Galactosylceramides with homogeneous acyl chains: the effect of acyl structure on intermolecular interactions occurring at the argon/buffered saline interface. *Thin Solid Films.* 244:860–864.

Applegate, K. R., and J. Glomset. 1991. Effect of acyl chain unsaturation on the packing of model diacylglycerols in simulated monolayers. *J. Lipid Res.* 32:1645–1655.

Aveldaño, M. I., and L. A. Horrocks. 1983. Quantitative release of fatty acids from lipids by a simple hydrolysis procedure. *J. Lipid Res.* 24: 1101–1105.

Barenholz, Y., and T. E. Thompson. 1980. Sphingomyelins in bilayers and biological membranes. *Biochim. Biophys. Acta.* 604:129–158.

Bartlett, G. R. 1959. Phosphorus assay in column chromatography. *J. Biol. Chem.* 234:466–469.

Bittman, R., C. R. Kasireddy, P. Mattjus, and J. P. Slotte. 1994. Interaction of cholesterol with sphingomyelin in monolayers and vesicles. *Biochemistry.* 33:11776–11781.

Blume, A. 1979. A comparative study of the phase transitions of phospholipid bilayers and monolayers. *Biochim. Biophys. Acta.* 557:32–44.

Brown, D. A. 1993. Interactions between GPI-anchored proteins and membrane lipids. *Trends Cell Biol.* 2:338–343.

Brown, D. A., and J. K. Rose. 1992. Sorting of GPI-anchored proteins to glycolipid-enriched membrane subdomains during transport to the apical cell surface. *Cell.* 68:533–544.

Bruzik, K. S. 1988. Conformation of the polar headgroups of sphingomyelin and its analogues. *Biochim. Biophys. Acta.* 939:316–326.

Bunow, M. R., and I. W. Levin. 1980. Molecular conformations of cerebrosides in bilayers determined by Raman spectroscopy. *Biophys. J.* 32:1007–1021.

Caille, A., D. Pink, F. de Verteuil, and M. J. Zuckermann. 1980. Theoretical models for quasi-two-dimensional mesomorphic monolayers and membrane bilayers. *Can. J. Phys.* 58:581–611.

Cevc, G., and D. Marsh. 1987. Phospholipid Bilayers. Wiley-Interscience, New York. 347–361.

Cleary, M. P., F. C. Phillips, and R. A. Morton. 1994. Liver, serum and adipose tissue fatty acid composition in suckling Zucker rats. *Lipids.* 29:753–758.

Cohen, R., Y. Barenholz, and A. Dagan. 1984. Preparation and characterization of well defined D-erythro sphingomyelins. *Chem. Phys. Lipids.* 35: 371–384.

Demel, R. A., W. S. M. Guerts von Kessel, and L. L. M. van Deenen. 1972. The properties of polyunsaturated lecithins in monolayers and liposomes and the interactions of these lecithins with cholesterol. *Biochim. Biophys. Acta.* 266:26–40.

Demel, R. A., W. S. M. Guerts von Kessel, R. F. A. Zwaal, B. Roelofson, and L. L. M. van Deenen. 1975. Relation between various phospholipase actions on human red cell membranes and the interfacial phospholipid pressure in monolayers. *Biochim. Biophys. Acta.* 406:97–107.

Demel, R. A., L. L. M. van Deenen, and B. Pethica. 1967. Monolayer interactions of phospholipids and cholesterol. *Biochim. Biophys. Acta.* 135:11–19.

Döbereiner, H.-G., J. Käs, D. Noppl, I. Sprenger, and E. Sackmann. 1993. Budding and fission of vesicles. *Biophys. J.* 65:1396–1403.

Evans, E., and D. Needham. 1987. Physical properties of surfactant bilayer membranes: thermal transitions, elasticity, rigidity, cohesion, and colloidal interactions. *J. Phys. Chem.* 91:4219–4228.

Evans, E., and W. Rawicz. 1990. Entropy-driven tension and bending in condensed-fluid membranes. *Phys. Rev. Lett.* 64:2094–2097.

Evans, E., and R. Waugh. 1977. Mechano-chemistry of closed, vesicular membrane systems. *J. Colloid Interface Sci.* 60:286–298.

Feng, S.-S., H. L. Brockman, and R. C. MacDonald. 1994. On osmotic-type equations of state for liquid-expanded monolayers of lipids at the air-water interface. *Langmuir.* 10:3188–3194.

Fiedler, K., T. Kobayashi, T. V. Kurzchalia, and K. Simons. 1993. Glycosphingolipid-enriched, detergent-insoluble complexes in protein sorting in epithelial cells. *Biochemistry.* 32:6365–6373.

Grönberg, L., Z. Ruan, R. Bittman, and J. P. Slotte. 1991. Interaction of cholesterol with synthetic sphingomyelin derivatives in mixed monolayers. *Biochemistry.* 30:10746–10754.

Hannun, Y. A. 1994. The sphingomyelin cycle and the second messenger function of ceramide. *J. Biol. Chem.* 269:3125–3128.

Hamilton, K. S., H. C. Jarrell, K. M. Briere, and C. W. M. Grant. 1993. Glycosphingolipid backbone conformation and behavior in cholesterol-containing phospholipid bilayers. *Biochemistry.* 32:4022–4028.

Hauser, H., and G. Poupart. 1992. Lipid structure. *In* The Structure of Biological Membranes. P. Yeagle, editor. CRC Press, Boca Raton, FL. 30–32.

Holte, L. L., S. A. Peter, T. M. Sinnwell, and K. Gawrisch. 1995. ^{2}H nuclear magnetic resonance order parameter profiles suggest a change of molecular shape for phosphatidylcholines containing a polyunsaturated acyl chain. *Biophys. J.* 68:2396–2403.

Jähnig, F. 1981. Critical effects from lipid-protein interaction in membranes. *Biophys. J.* 36:329–345.

Johnston, D. S., and D. Chapman. 1988. The properties of brain galactocerebroside monolayers. *Biochim. Biophys. Acta.* 937:10–22.

Kwok, R., and E. Evans. 1981. Thermoelasticity of large lecithin bilayer vesicles. *Biophys. J.* 35:637–652,

Lapidot, Y., S. Rappoport, and Y. Wolman. 1967. Use of esters of N-hydroxysuccinimide in the synthesis of N-acylaminoacids. *J. Lipid Res.* 8:142–145.

Lis, L. J., M. McAlister, N. Fuller, R. P. Rand, and V. A. Parsegian. 1982. Measurement of the lateral compressibility of several phospholipid bilayers. *Biophys. J.* 37:667–672.

Lund-Katz, S., H. M. Laboda, L. R. McLean, and M. C. Phillips. 1988. Influence of molecular packing and phospholipid type on the rates of cholesterol exchange. *Biochemistry.* 27:3416–3423.

Marcelja, S. 1974. Chain ordering in liquid crystals. II. Structure of bilayer membranes. *Biochim. Biophys. Acta.* 367:165–176.

Mason, J. T., A. V. Broccoli, and C. Huang. 1981. A method for the synthesis of isomerically pure saturated mixed chain phosphatidylcholines. *Anal. Biochem.* 113:96–101.

McIntosh, T. J., S. A. Simon, D. Needham, and C. C. Huang. 1992. Structure and cohesive properties of sphingomyelin/cholesterol bilayers. *Biochemistry.* 31:315–328.

Mouritsen, O. G., J. H. Ipsen, and M. J. Zuckermann. 1989. Lateral density fluctuations in the chain-melting phase transition of lipid monolayers. *J. Colloid Interface Sci.* 129:32–40.

Müller-Landau, F., and D. A. Cadenhead. 1979. Molecular packing in steroid-lecithin monolayers. Part II. Mixed films of cholesterol with dipalmitoylphosphatidylcholine and tetradecanoic acid. *Chem. Phys. Lipids.* 25:315–328.

Nagle, J. F. 1980. Theory of the main lipid bilayer phase transition. *Annu. Rev. Phys. Chem.* 31:157–195.

Nagle, J. F., and H. L. Scott, Jr. 1978. Lateral compressibility of lipid mono- and bilayers: theory of membrane permeability. *Biochim. Biophys. Acta.* 513:236–243.

Needham, D., T. J. McIntosh, and E. Evans. 1988. Thermomechanical and transition properties of dimyristoylphosphatidylcholine/cholesterol bilayers. *Biochemistry.* 27:4668–4673.

Needham, D., and R. S. Nunn. 1990. Elastic deformation and failure of lipid bilayer membranes containing cholesterol. *Biophys. J.* 58: 997–1009.

Nieva, J. L., R. Bron, J. Corver, and J. Wilschut. 1994. Membrane fusion of Semliki forest virus requires sphingolipids in the target membrane. *EMBO J.* 13:2797–2804.

Parsegian, V. A., N. Fuller, and R. P. Rand. 1979. Measured work of deformation and repulsion of lecithin bilayers. *Proc. Natl. Acad. Sci. USA.* 76:2750–2754.

Phillips, M. C., and D. Chapman. 1968. Monolayer characteristics of saturated 1,2-diacyl phosphatidylcholines (lecithins) and phosphatidylethanolamines at the air-water interface. *Biochim. Biophys. Acta.* 163:301–313.

Phillips, M. C., D. E. Graham, and H. Hauser. 1975. Lateral compressibility and penetration into phospholipid monolayers and bilayer membranes. *Nature.* 254:154–156.

Phillips, M. C., and H. Hauser. 1974. Spreading of solid glycerides and phospholipids at the air-water interface. *J. Colloid Interface Sci.* 49: 31–39.

Pink, D. A., A. L. MacDonald, and B. Quinn. 1988. Anisotropic interactions in hydrated cerebrosides: a theoretical model of stable and metastable states and hydrogen-bond formation. *Chem. Phys. Lipids.* 47: 83–95.

Radin, N. S. 1974. Preparation of psychosines (1-O-hexosyl sphingosine) from cerebrosides. *Lipids.* 9:358–360.

Rand, R. P., N. Fuller, V. A. Parsegian, and D. C. Rau. 1988. Variation in hydration forces between neutral phospholipid bilayers: evidence for hydration attraction. *Biochemistry.* 27:7711–7722.

Rand, R. P., and V. A. Parsegian. 1992. The forces between interacting bilayer membranes and the hydration of phospholipid assemblies. *In* The Structure of Biological Membranes. P. Yeagle, editor. CRC Press, Boca Raton, FL. 251–306.

Schwarzmann, G., and K. Sandhoff. 1987. Lysogangliosides: synthesis and use in preparing labeled gangliosides. *Methods Enzymol.* 138:319–341.

Selinger, Z., and Y. Lapidot. 1966. Synthesis of fatty acid anhydrides by reaction with dicyclohexylcarbodiimide. *J. Lipid Res.* 7:174–175.

Slotte, J. P., A. L. Ostman, E. R. Kumar, and R. Bittman. 1993. Cholesterol interacts with lactosyl and maltosyl cerebrosides but not with glucosyl or galactosyl cerebrosides in mixed monolayers. *Biochemistry.* 32: 7886–7892.

Smaby, J. M., and H. L. Brockman. 1991. Evaluation of models for surface pressure-area behavior of liquid-expanded monolayers. *Langmuir.* 7:1031–1034.

Smaby, J. M., H. L. Brockman, and R. E. Brown. 1994. Cholesterol's interfacial interactions with sphingomyelins and phosphatidylcholines: hydrocarbon chain structure determines the magnitude of condensation. *Biochemistry.* 33:9135–9142.

Smaby, J. M., H. L. Brockman, and R. E. Brown. 1995. Interfacial compressibility changes induced by cholesterol's interactions with sphingomyelins and phosphatidylcholines. *Biophys. J.* 68:A98.

Smaby, J. M., A. Hermetter, P. C. Schmid, F. Paltauf, and H. L. Brockman. 1983. Packing of ether and ester phospholipids in monolayers: evidence for hydrogen-bonded water at the sn-1 acyl group of phosphatidylcholines. *Biochemistry.* 22:5808–5813.

Thompson, T. E., and T. W. Tillack. 1985. Organization of glycosphingolipids in bilayers and plasma membranes of mammalian cells. *Annu. Rev. Biophys. Biophys. Chem.* 14:361–386.

Yedgar, S., R. Cohen, S. Gatt, and Y. Barenholz. 1982. Hydrolysis of monomolecular layers of synthetic sphingomyelins by sphingomyelinase of *Staphylococcus aureus. Biochem. J.* 201:597–603.

Zuckermann, M. J., J. H. Ipsen, and O. G. Mouritsen. 1993. Theoretical studies of the phase behavior of lipid bilayers containing cholesterol. *In* Cholesterol in Model Membranes. L. Finegold, editor. CRC Press, Boca Raton, FL. 223–257.